Chapter 5

Water Productivity Modeling by Remote Sensing in the Semiarid Region of Minas Gerais State, Brazil

Antônio Heriberto de Castro Teixeira,
Fúlvio R. Simão, Janice F. Leivas, Reinaldo L. Gomide,
João B.R. da S. Reis, Mauro K. Kobayashi and
Flávio G. Oliveira

Additional information is available at the end of the chapter

http://dx.doi.org/10.5772/intechopen.72105

Abstract

This chapter aimed to demonstrate the potential of monitoring water and vegetation parameters by combining weather and satellite measurements in mixed agroecosystems in the semiarid region of the northern Minas Gerais state, Southeast Brazil. Soil moisture indices and water productivity components were quantified with Landsat 8 images under different hydrological conditions along the year 2015. The surface resistance to the water fluxes (r_s) performed better than the ratio of actual to the reference evapotranspiration (ET_r) to detect soil moisture conditions. The mean pixel values for actual evapotranspiration (ET), biomass production (BIO), and water productivity based on evapotranspiration (WP), for irrigated crops (IC), ranged respectively from 2.5 ± 1.3 to 4.1 ± 1.6 mm d^{-1}; 78 ± 62 to 132 ± 64 kg ha^{-1} d^{-1}; and from 2.2 ± 0.8 to 3.3 ± 0.9 kg m^{-3}. The corresponding ranges for natural vegetation (NV) were 0.1 ± 0.2 to 1.9 ± 1.3 mm d^{-1}; 1 ± 1 to 44 ± 42 kg ha^{-1} d^{-1}, and 0.6 ± 0.3 to 1.8 ± 0.8 kg m^{-3}. The incremental values, resulting from the replacement of natural species by agricultural crops, were respectively 2.7 mm d^{-1} and 83 kg ha d^{-1}. However, this replacement increased water productivity based on evapotranspiration (WP) by 264% during the studied year, what should be considered in land use and climate change studies in the Brazilian semiarid region.

Keywords: SAFER, SUREAL, soil moisture, evapotranspiration, biomass production

1. Introduction

In the semiarid region of the northern Minas Gerais state, Southeast Brazil, the availability of water resources for irrigation is responsible for the rural economy growth. The main commercial crops are fruits and sugar cane; however, one of the main consequences of this development is

that other water users are competing with those from the agricultural sectors. The Jaíba irrigation scheme has a total area of 107,600 ha, being 65,800 ha irrigable, involving Jaíba and Matias Cardoso counties. The Gorotuba irrigation scheme has a total area of 11,280 ha, from which 4886 are irrigable, involving the counties of Janaúba, Nova Porteirinha, and Riacho dos Machados [1].

The irrigation schemes make the north of Minas an important agricultural growing region, because of the rapid development of the irrigation technologies. Under the actual climate and land-use change scenarios in the Brazilian semiarid region, the use of remote sensing from satellites, for quantifying the large-scale soil moisture and water productivity components in mixed agroecosystems, is strongly relevant. These knowledges provide valuable information for the water resource conservation practices without lowering the agricultural production. To meet this goal, there is the need for large scale quantifying both actual evapotranspiration (ET) and biomass production (BIO).

Actual evapotranspiration (ET) is critically important because of its relation with yield in all agroecosystems. On the one hand, it is the main water use for agriculture. On the other hand, increase in evapotranspiration rates results in less water availability for ecological and human uses in hydrological basins. The difficulties of acquiring large-scale water fluxes throughout field measurements in semiarid environments highlighted the use of remote sensing from satellites, together with agrometeorological stations [2, 3].

The Simple Algorithm for Evapotranspiration Retrieving (SAFER) model, for energy radiation and energy balance accounting, was developed and validated in the Brazilian semiarid region through simultaneous Landsat and field measurements, involving strong contrasting hydrological conditions and agroecosystem types during several years [4, 5].

Remote sensing from satellites is also an effective tool for large-scale biomass production estimations. The radiation use efficiency (RUE) model proposed by Monteith [6] has acceptable accuracy for this purpose, providing spatial and temporal information of vegetation locations and plant status [7].

A third model, the Surface Resistance Algorithm (SUREAL), was elaborated to calculate the surface resistance to water fluxes (r_s), a soil moisture index, with field and Landsat data [4, 5], for classifying mixed agroecosystems into irrigated crops (IC) and natural vegetation (NV) [8].

All the referred models are applied together with a net of agrometeorological stations in this chapter to retrieve large-scale water and vegetation indices, highlighting the combination of remote sensing algorithms as suitable tools for using together with weather data. The study aimed to apply these tools for subsidizing large-scale water productivity assessments in irrigated crops and natural vegetation under the semiarid conditions of Minas Gerais state, Southeast Brazil.

2. Materials and methods

2.1. Study area and data set

Figure 1 shows the location of the study area with the county divisions and the agrometeorological stations used in the semiarid region of the north of Minas Gerais state, Southeast Brazil.

http://dx.doi.org/10.5772/intechopen.72105

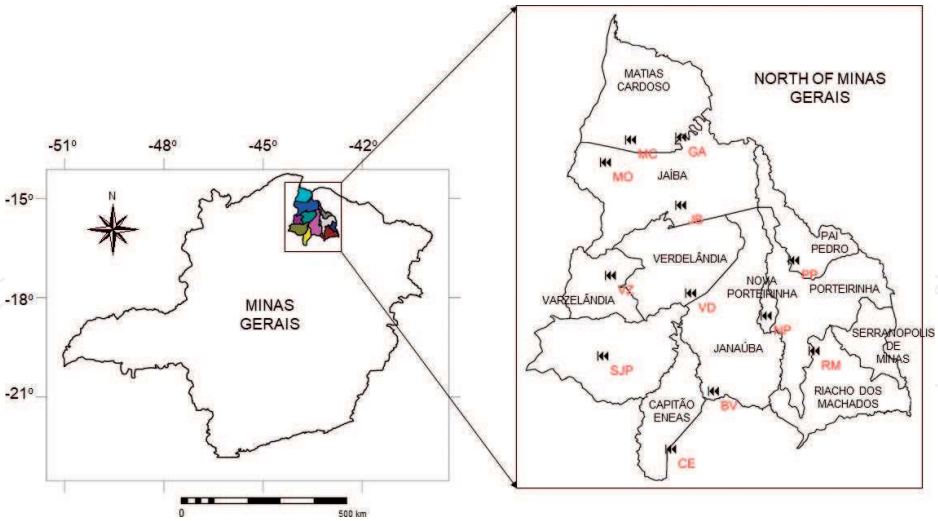

Figure 1. Location of the study area and agrometeorological stations inside the counties under the semiarid conditions of the north of Minas Gerais state, Southeast Brazil.

The agrometeorological stations are Mocambinho (MC), Matias Cardoso (MC), Gameleiras (GA), Jaíba (JB), Varzelândia (VZ), Verdelândia (VD), Pai Pedro (PP), Nova Porteirinha (NP), São João da Ponte (SJP), Riacho dos Machado (RM), Bela Vista (BV), and Capitão Eneas (CE).

The predominant vegetation cover in the semiarid region of the northern Minas Gerais state, Southeast Brazil, is classified as "Cerrado," "Caatinga," and transitions [9], and the main hydrological basins are São Francisco and Jequitinhonha [10].

According to Lumbreras et al. [11], long-term rainfall is below 900 mm $yr.^{-1}$, concentrated in the first and the last 3 months of the year. Thermal conditions are characterized by high air temperature (T_a), with averages of 24°C and maximums between 31 and 32°C, occurring from September to October, when the sun is around the zenith position in the region. The coldest period is from June to July, solstice period in the Southern hemisphere, when the minimums are from 14 to 17°C.

2.2. Large-scale soil moisture and water productivity modeling

The Landsat 8 images involved the orbit 218 and the points 70 and 71, which mosaics covered different hydrological conditions along the year 2015, represented by the Days of the Year (DOY) 019 (January 19), 163 (June 12), 259 (September 16) and 307 (November 03). **Figure 2** shows the steps for modeling the soil moisture indices and water productivity components throughout the Simple Algorithm for Evapotranspiration Retrieving (SAFER), Radiation Use Efficiency (RUE), and Surface Resistance Algorithm (SUREAL) models.

According to **Figure 2**, from the Digital Numbers (DN), the spectral radiances for each band (L_{band}) are calculated:

$$L_{band} = aDN + b \quad (1)$$

where a and b are regression coefficients given in the metadata file [12].

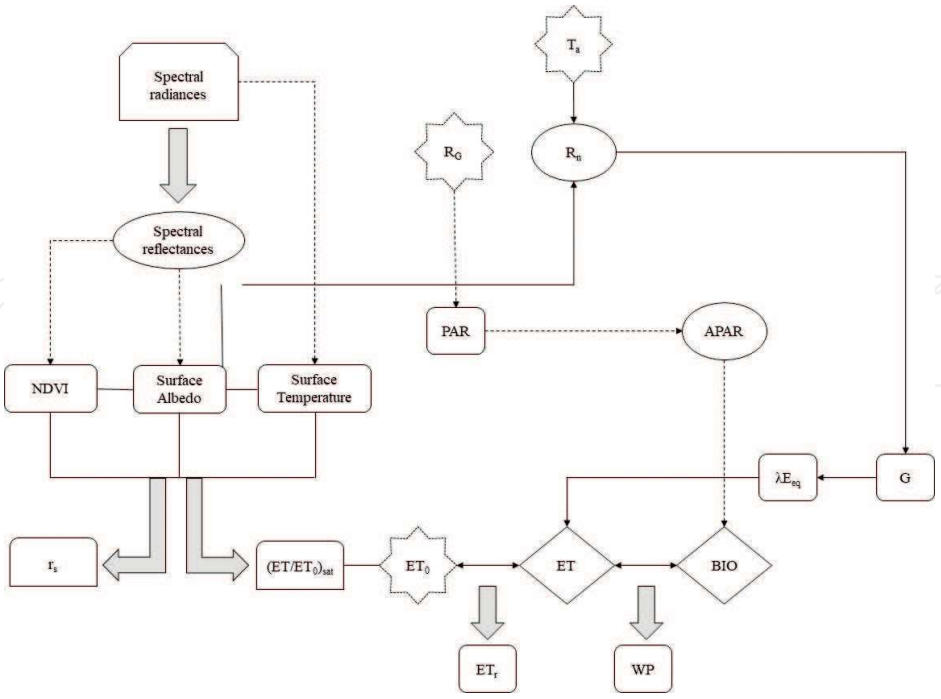

Figure 2. Flow chart for modeling soil moisture indices and water productivity components throughout application of the Simple Algorithm for Evapotranspiration Retrieving (SAFER), Radiation Use Efficiency (RUE), and Surface Resistance Algorithm (SUREAL) models to Landsat 8 images together with agrometeorological data.

The albedo at the top of the atmosphere for each band (αt_{band}) of the satellite sensor was calculated as:

$$\alpha\, t_{band} = \frac{L_{band}\, \pi d^2}{Rt_{band} \cos\varphi} \tag{2}$$

where L_{band} is in W m^{-2} sr^{-1} μm^{-1}, d is the relative earth-sun distance, Rt_{band} is the mean solar irradiance at the top of the atmosphere for each band (W m^{-2} μm^{-1}), and φ is the solar zenith angle [3].

Following Teixeira et al. [3], the broadband albedo at the top of the atmosphere (αt) was calculated as the total sum of the different narrow-band αt_{band} values according to the weights for each band (w_b).

$$\alpha t = \sum w_{band}\, \alpha t_{band} \tag{3}$$

where the w_{band} values were computed as the ratio of the amount of the incoming shortwave radiation from the sun at the top of the atmosphere in a particular band and the sum for all the bands.

The spectral radiances from the thermal bands 10 (L_{10}) and 11 (L_{11}) were used to calculate the radiometric temperatures (T_{band}) applying the Plank's law:

$$T_{band} = \frac{K_2}{\ln\left(\frac{K_1}{L_{band}+1}\right)}, \tag{4}$$

where K_1 (774.89 and 480.89) and K_2 (1321.08 and 1201.14) the conversion coefficients for the bands 10 and 11, respectively.

The average T_{band} value from the two bands was considered as the brightness temperature (T_{bright}); however, conditional functions were used when one of the bands 10 or 11 presented pixel value problems to retrieve only one band Plank's result for T_{bright}.

Both αt and T_{bright} were corrected atmospherically for acquiring the albedo (α_0) and temperature (T_0) surface instantaneous values, by regression equations determined from previous simultaneous Landsat and field measurements. Other regressions between the instantaneous and daily values were also applied to upscale the satellite overpass to the 24-h α_0 and T_0 values [3].

The Normalized Difference Vegetation Index (NDVI) is a measure of the vegetation amount at the surface:

$$NDVI = \frac{\alpha t_{(nir)} - \alpha t_{(red)}}{\alpha t_{(nir)} + \alpha t_{(red)}} \tag{5}$$

where αt_{nir} and αt_{red} represent the albedo at the top of the atmosphere over the ranges of wavelengths in the near infrared (subscript *nir*) and red (subscript *red*) regions of the solar spectrum, which for Landsat 8 satellite are the bands 5 and 4, respectively.

The satellite overpass (subscript *sat*) values for the ratio of actual evapotranspiration (ET) to the reference evapotranspiration (ET_0) were modeled as [5]:

$$\left(\frac{ET}{ET_0}\right)_{sat} = \exp\left[a_{sf} + b_{sf}\left(\frac{T_0}{\alpha_0 NDVI}\right)\right] \tag{6}$$

where a_{sf} and b_{sf} are regression coefficients of 1.8 and −0.008, for the Brazilian semiarid conditions.

Eq. 6 does not work for water bodies (i.e., NDVI <0). In these situations, the concept of equilibrium evapotranspiration (ET_{eq}) is incorporated into the Simple Algorithm for Evapotranspiration Retrieving (SAFER) algorithm [13], applying conditional functions to negative NDVI values. Then, the large-scale actual evapotranspiration (ET) values are obtained as:

$$ET = \left(\frac{ET}{ET_0}\right)_{sat} ET_0 \text{ or } 0.035\left(\frac{s(R_n - G)}{s + \gamma}\right) \tag{7}$$

where s is the inclination of the curve relating the saturation vapor pressure (e_s) and the air temperature (T_a), R_n is the net radiation, G is the ground heat flux, and γ is the psychrometric constant.

Net radiation (R_n) can be described through the 24-h values of net shortwave radiation, with a correction term for net longwave radiation [4]:

$$R_n = (1 - \alpha_0)R_G - a_L\tau \tag{8}$$

where a_L is the regression coefficient of the relationship between net long wave radiation and atmospheric transmissivity (τ) on a daily scale.

For ground heat flux (G), the equation derived by Teixeira [5] was used:

$$\frac{G}{R_n} = a_G \exp(b_G \alpha_0) \tag{9}$$

where a_G and b_G (3.98; −25.47) are the regression coefficients.

A soil moisture index (ET_r) is considered by recalculating the ratio of the actual (ET) to reference (ET_0) evapotranspiration on a daily scale:

$$ET_r = \frac{ET}{ET_0} \tag{10}$$

For biomass production (BIO) calculations, the radiation use efficiency (RUE) model was used, introducing the soil moisture effects through the daily ratio of actual to reference evapotranspiration (ET_r):

$$BIO = \varepsilon_{max} ET_r PAR_{abs} 0.864 \tag{11}$$

where ε_{max} is the maximum radiation efficiency use, PAR_{abs} is the absorbed photosynthetically active radiation, and 0.864 is a unit conversion factor.

The absorbed photosynthetically active radiation (PAR_{abs}) was estimated as function of the Normalized Difference Vegetation Index (NDVI) and the incident photosynthetically active radiation (PAR_{inc}), which in turn is considered a fraction of the global solar radiation (R_G):

$$PAR_{abs} = (a_{fr} NDVI + b_{fr}) PAR_{inc} \tag{12}$$

where the coefficients a_{fr} and b_{fr} were considered 1.257 and −0.161 [14].

As another index, the surface resistance to the water fluxes (r_s) was used to picture the soil moisture conditions, but also for classifying the vegetation, into irrigated crops (IC) and natural vegetation (NV), throughout the surface resistance algorithm (SUREAL) model [5]:

$$r_s = \exp\left[a_r \left(\frac{T_0}{\alpha_0}\right)(1 - NDVI) + b_r\right] \tag{13}$$

where a_r and b_r are the regression coefficients of 0.04 and 2.72 for the Brazilian semiarid conditions.

3. Results and discussion

3.1. Large-scale weather conditions

Figure 3 presents the tendencies of the fortnight mean pixel values for precipitation (P) and reference evapotranspiration (ET_0) resulted from the weather interpolation process in the study area, including the periods before, during, and after the satellite image acquisitions. Weather conditions during these periods will affect the image process results.

http://dx.doi.org/10.5772/intechopen.72105

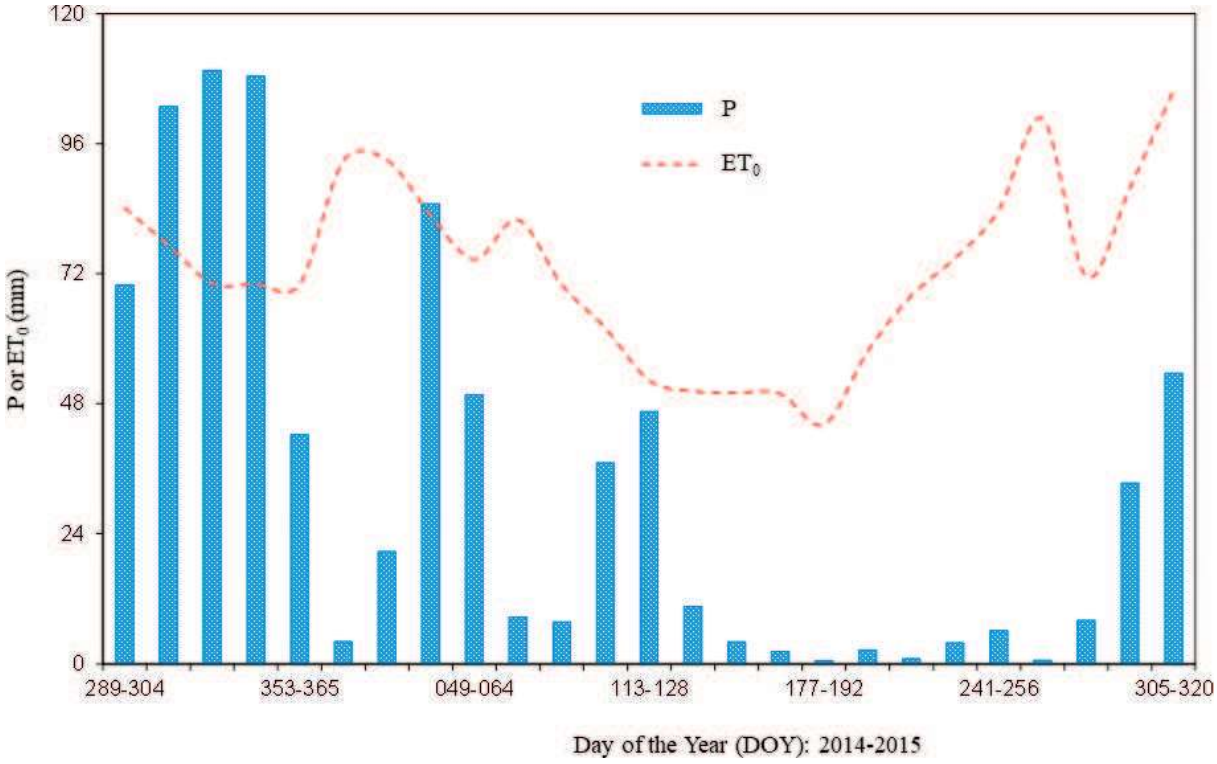

Figure 3. Climatic water balance components in the semiarid region of the northern Minas Gerais state, involving the fortnight periods from 2014 to 2015, before, during, and after the image acquisitions: precipitation (P) and reference evapotranspiration (ET_0).

Because of the semiarid characteristics of the study region and the proximity of the equator, precipitation (P) was much more variable than reference evapotranspiration (ET_0). Rainfall concentrations were at the start and at the end of the years, in agreement with Lumbreras et al. [11]. The driest period, with precipitation (P) fortnight values below 5 mm, was from Day of the Year (DOY) 160 to 289 in 2015, lower than 10% of the reference evapotranspiration (ET_0). However, one can see other natural water scarcity events, one at the start of January and from Day of the Year (DOY) 064 to 097, even inside the normal rainy season conditions of the region.

Regarding the reference evapotranspiration (ET_0) values, the largest atmospheric demands were at the end of 2015, when the fortnight values were higher than 80 mm. Under these situations, the sun was around its zenith position with the sky presenting low cloud cover. Under the conditions of high both precipitation (P) and reference evapotranspiration (ET_0), during the start and at the end of year, all agroecosystems, irrigated crops (IC) and natural vegetation (NV) were in favor for large actual evapotranspiration (ET) and biomass production (BIO) rates.

3.2. Large-scale soil moisture indices

Figure 4 shows the spatial distribution for the actual to reference evapotranspiration ratio (ET_r) and its daily average values, involving different hydrological conditions and agroecosystems along the year 2015, in the semiarid region of the north of Minas Gerais state, Southeast Brazil.

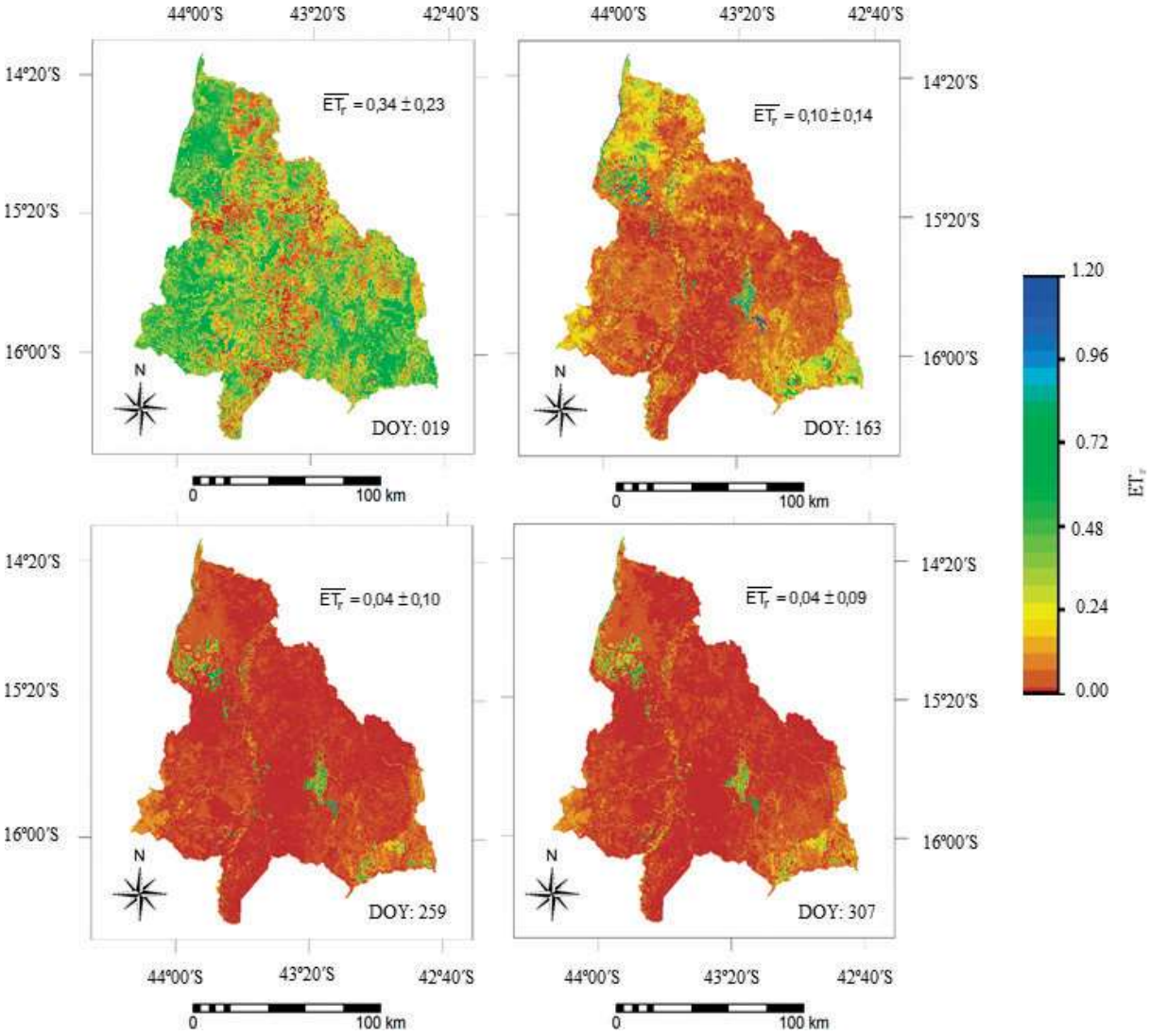

Figure 4. Spatial distribution of the daily values for the ratio of actual evapotranspiration – ET to the reference evapotranspiration – ET_0 (ET_r), involving different hydrological conditions and agroecosystems along the year 2015, in the north of Minas Gerais state, Southeast Brazil. DOY is the Day of the Year, and the over bars mean averages showed together with the standard deviation (SD).

The spatial and temporal variations, the actual (ET) to reference evapotranspiration (ET_0) ratio (ET_r), along the year 2015 are evident, confirming the sensibility of the Simple Algorithm for Evapotranspiration Retrieving (SAFER) model to picture the soil moisture involving different hydrological conditions and agroecosystems. The spatial variations of this ratio are much strongly noticed when comparing the images representative of the rainy period (DOY 027, January 29) when some well irrigated areas presented values above 1.00, against that for the driest one of DOY 307 (November 03), when some pixels reach to 0.00 values in natural species (**Figures 3** and **4**). The highest values for Jaíba, Nova Porteirinha, and Riacho dos Machados counties during the climatically driest periods (**Figures 1** and **4**) may be attributed to largest concentrations of irrigated areas.

In well-irrigated crops, the actual to reference evapotranspiration ratio (ET_r) values, called in this case the crop coefficient (K_c), may be used for estimating the water requirements at different spatial scales [15]. On the other hand, in natural vegetation, this ratio characterizes the degree of the water stress in the plant root zones [16].

In a temperate desert steppe of the Inner Mongolia, China, the seasonal actual to reference evapotranspiration ratio (ET_r) ranged from mean daily values of 0.16 to maximum of 0.75 [17], similar to several situations of the current study. However, Lu et al. [16], in the same Chinese region, found this ratio higher than 1.00 for six different ecosystems, while it was inside a range from 0.47 to 0.92 in a non-irrigated pasture site in Florida, USA [18].

The most important variables for the actual to reference evapotranspiration ratio (ET_r) variations in a reed marsh in the Northeast China were attributed to air temperature, air humidity, and the available energy [19]. In the Brazilian semiarid conditions, previous rainy seasons were the most significant reason for the highest values of this ratio, increasing the soil moisture in the subsequent periods. However, the values of this soil moisture index in natural ecosystems also depend on the stomatal regulation and plant adaptation to water scarcity conditions [20].

In this chapter, the surface resistance to the water fluxes (r_s) is considered for both, being a candidate to picture the soil moisture conditions and to classify the agroecosystems into irrigated crops (IC) and natural vegetation (NV). As lower are its values, higher is the root zone moisture [3].

Figure 5 shows the spatial distribution for the surface resistance to water fluxes (r_s) and its average daily values, involving different hydrological conditions and agroecosystems along the year 2015, in semiarid region of the north of Minas Gerais state, Southeast Brazil.

The spatial and temporal variations of the surface resistance to water fluxes (r_s) are also clear along the year 2015, confirming the sensibility of the Surface Resistance Algorithm (SUREAL) model for detecting differences in soil moisture conditions among agroecosystems under semiarid conditions. As in the case of the actual to reference evapotranspiration ratio (ET_r), the spatial soil moisture differences are also strongly noticed comparing the representative images for the rainy period (DOY 019–January 19) against that for the driest conditions (DOY 307–November 03). However, it is clear that the surface resistance to water fluxes (r_s) detects the soil moisture differences stronger than the actual to reference evapotranspiration ratio (ET_r) when analyzing the images of DOY 259 (September 19) and 307 (November 03) from **Figures 4** and **5**.

Then, the surface resistance to water fluxes (r_s) image during the driest conditions of DOY 259 was taken for the vegetation classification. In this image, pixel values below 800 s m^{-1} and the Normalized Difference Vegetation Index (NDVI) above or equal to 0.30 were considered irrigated crops (IC), while those with values between 1000 and 10,000 s m^{-1} and the Normalized Difference Vegetation Index (NDVI) below 0.30 were considered natural vegetation (NV). The high end of this last range was included to filter rocks and buildings [3]. The lowest values of the surface resistance to water fluxes (r_s) in vegetation indicate good soil moisture conditions, while the highest ones are related to water stress in all agroecosystems.

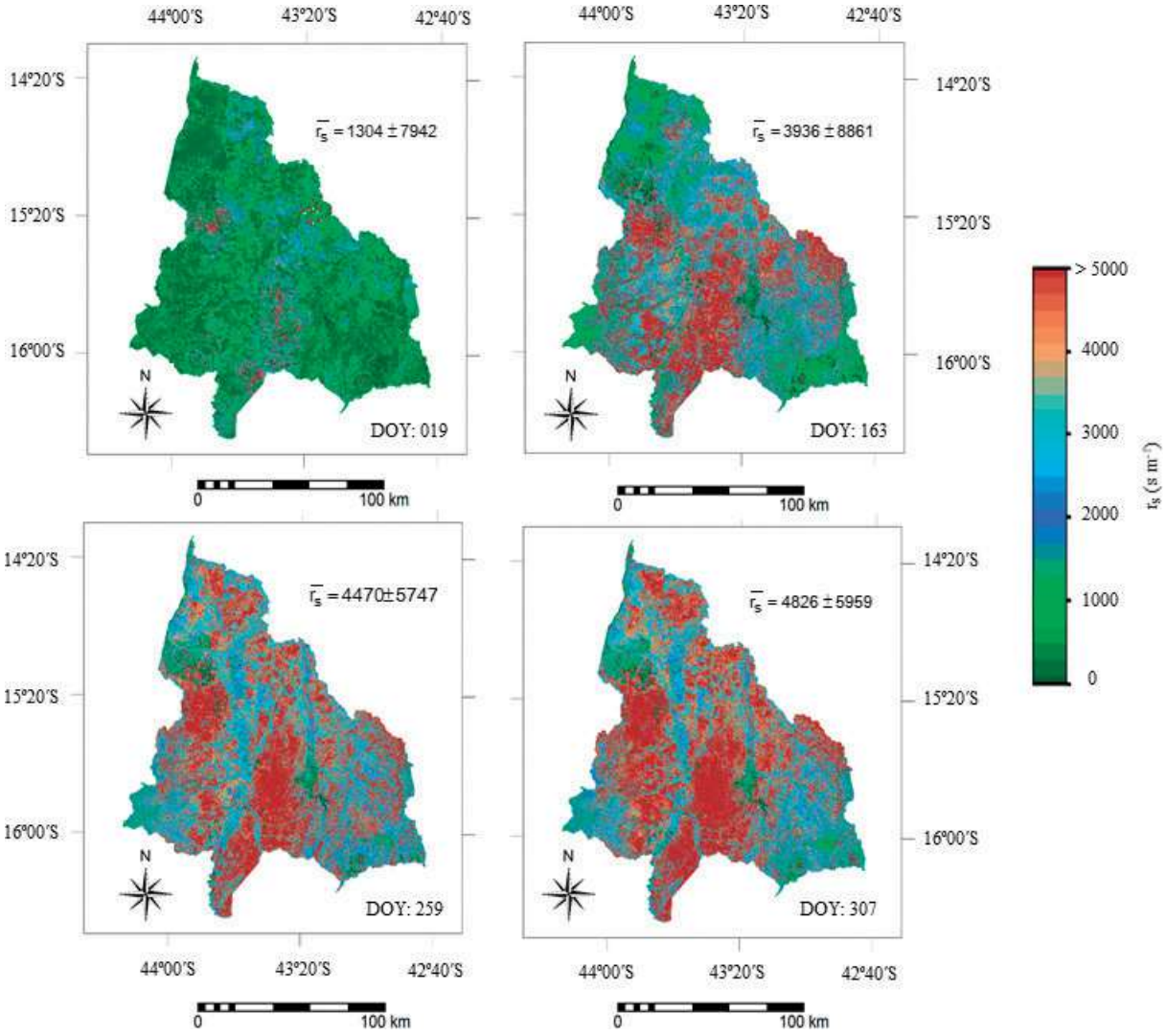

Figure 5. Spatial distribution for the surface resistance to water fluxes (r_s), under different hydrological conditions and agroecosystems along the year 2015, in the north of Minas Gerais state, Southeast Brazil. DOY is the Day of the Year, and the over bars means averages showed together with standard deviation (SD).

3.3. Large-scale water productivity parameters

Figure 6 shows the spatial distribution and the average daily values for actual evapotranspiration (ET) and biomass production (BIO) for irrigated crops (IC) and natural vegetations (NV), under different hydrological conditions along the year 2015, in the north of Minas Gerais state, Southeast Brazil.

The spatial and temporal variations for actual evapotranspiration (ET) (**Figure 6a**) and biomass production (BIO) (**Figure 6b**) are both strong. This is noticed mainly when comparing the wettest conditions (represented by the image of DOY 019—January 19) with the driest ones (represented by the image of DOY 259—September 16), where the pixels with the high values represent irrigated crops (IC). The largest rates for both water productivity parameters occurred during the

http://dx.doi.org/10.5772/intechopen.72105

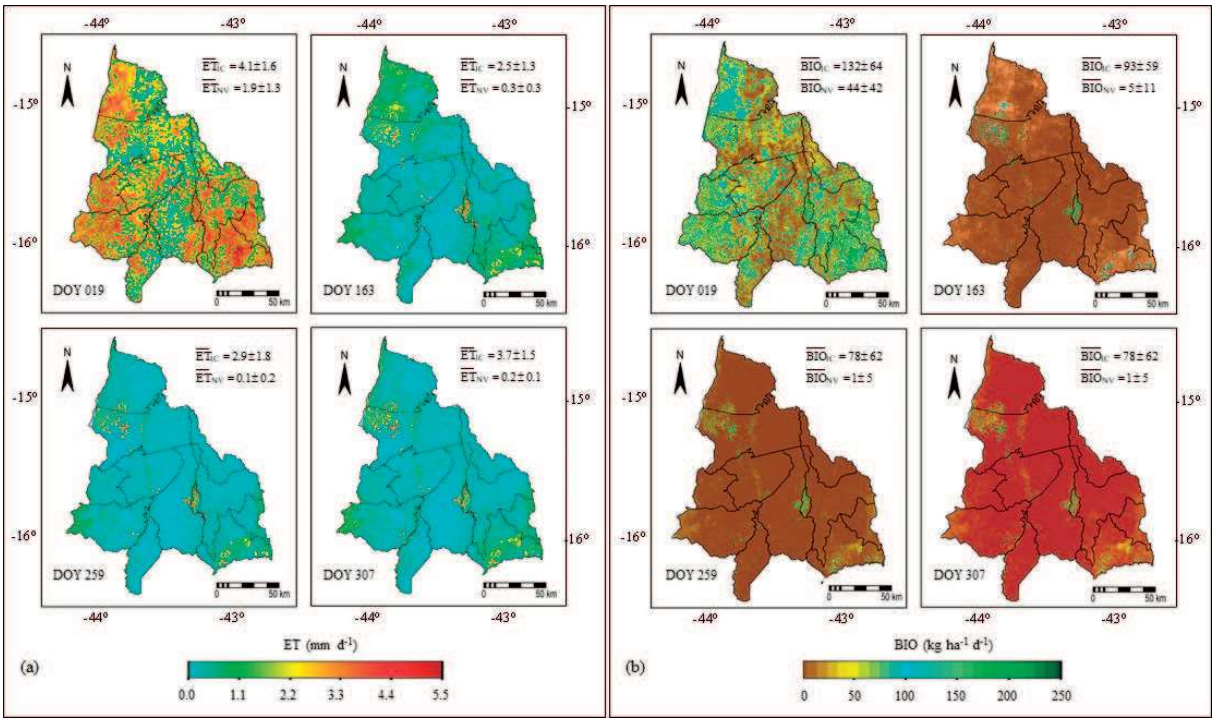

Figure 6. Spatial distribution and the daily average values for the water productivity parameters, under different hydrological conditions along the year 2015, in the north of Minas Gerais state, Southeast Brazil. (a) Actual evapotranspiration (ET) and (b) biomass production (BIO). DOY is the Day of the Year and the over bars means averages for irrigated crops (IC) and natural vegetation (NV) showed together with standard deviations (SD).

rainy period, when the accumulated precipitation (P) favored the natural species, while besides the rainfall water supply, irrigated crops were beneficed with supplementary irrigation.

The lowest actual evapotranspiration (ET) and standard deviation (SD) values for irrigated crops (IC) were soon after the rainy period, conditions represented by the image of DOY 163 (June 12). For biomass production (BIO), they were during the climatically driest conditions, represented by the image of DOY 259 (September 16), however with the lowest spatial variations in November (DOY 307). Considering the natural vegetation ecosystem (NV), the highest both actual evapotranspiration (ET) and biomass production (BIO) values occurred during the rainy period, represented by the image of DOY 019 (January 19), while the lowest ones were during the climatically driest period (DOY 259, September 16), because of the low soil moisture conditions promoting short vegetative development of natural species. Under these last conditions, the native plants are in dormancy stage, closing stomata what limit both transpiration and photosynthesis, and in general, crops are regularly daily irrigated, increasing the water productivity parameters.

The average pixel values for actual evapotranspiration (ET) and biomass production (BIO), in irrigated crops (IC), ranged respectively from 2.5 ± 1.3 to 4.1 ± 1.6 mm d^{-1} and from 78 ± 62 to 132 ± 64 kg ha^{-1} d^{-1}. The corresponding ranges for natural vegetation (NV) were 0.1 ± 0.2 to 1.9 ± 1.3 mm d^{-1} and de 1 ± 1 to 44 ± 42 kg ha^{-1} d^{-1}. Leivas et al. [2] reported maximum actual evapotranspiration (ET) values of 3.5 ± 1.0 mm d^{-1} in the Jaíba irrigation scheme. In the Petrolina/Juazeiro agricultural growing region, under the semiarid conditions of the São

Francisco river basin, Teixeira et al. [7] found maximum values of biomass production (BIO) of 100 and 46 kg ha^{-1} d^{-1} in irrigated crops (IC) and natural vegetation (NV) agroecosystems, respectively. These differences, regarding the results in this chapter, may be related, in part, to the lower spatial resolution of the MODIS images used in the previous studies, in comparison with that for the Landsat 8 in the current research.

While along the year, the values for actual evapotranspiration (ET) and biomass production (BIO) were progressively declining, reaching close to zero in November (DOY 307) in the natural vegetation (NV) ecosystem, in irrigated crops (IC), they were always above 2.5 mm d^{-1} and 78 kg ha d^{-1}, respectively. In an annual scale, the incremental rates resulting from the replacement of natural species by irrigated crops were 2.7 mm d^{-1} and 83 kg ha d^{-1}.

The largest both actual evapotranspiration (ET) and biomass production (BIO) were for the Jaíba and Matias Cardoso counties (**Figures 1** and **6**), because of the irrigation water availability in the Jaíba irrigation scheme, from the São Francisco river. Highlights in the region are also for Nova Porteirinha and Janaúba counties, inside the Gorotuba irrigation scheme, but in this last case, the dam Bico da Pedra is the water source. These irrigation schemes concentrate mainly irrigated fruit cops and sugar cane. The Riacho dos Machados county also presents some areas with high actual evapotranspiration (ET) and biomass production (BIO), being these large values probably related to cattle and family farms, with the main water sources from the Vacaria River and the Samambaia Stream.

Figure 7 shows the spatial distribution and the average daily values for the water productivity based on evapotranspiration (WP) for irrigated crops (IC) and natural vegetation (NV), under different hydrological conditions along the year 2015, in the north of Minas Gerais state, Southeast Brazil.

In the case of the water productivity based on evapotranspiration (WP), considered as the ratio of biomass production (BIO) to actual evapotranspiration (ET), the largest values and spatial variations for irrigated crops (IC) were in June (representative image of DOY 163), period of optimum crop root-zone moisture conditions, happening soon after the rainy period. On the other hand, inside the rainy period (conditions represented by the image of DOY 019), happened the highest values for the natural vegetation (NV) ecosystem. The large spatial variations indicated different soil moisture and vegetation conditions in natural species and heterogeneity on crop stages in irrigated crops. More uniformity on the values of water productivity based on evapotranspiration (WP) was for the natural vegetation (NV) ecosystem, evidenced by the lower standard deviations when compared to the irrigated crops (IC) agroecosystem.

The seasonal values of the water productivity based on evapotranspiration (WP) for the irrigated crops (IC) agroecosystem ranged from 2.2 ± 0.8 to 3.3 ± 0.9 kg m^{-3}. The corresponding range for the natural vegetation (NV) ecosystem was from 0.6 ± 0.3 to 1.8 ± 0.8 kg m^{-3}. These values when multiplied by the harvest index (HI) give the crop water productivity (CWP). Reported harvest index (HI) values were around 0.60 and 0.80 for vineyards and mango orchard under the semiarid conditions of Northeast Brazil, retrieving crop water productivity (CWP) values of 2.8 and 3.4 kg m^{-3} [21]. The maximum values for water productivity based on evapotranspiration (WP) in the current study when multiplied by these harvest indexes (HI) are lower, being the probable reason the water allocation restriction for irrigation schemes during the drought events in the year 2015.

http://dx.doi.org/10.5772/intechopen.72105

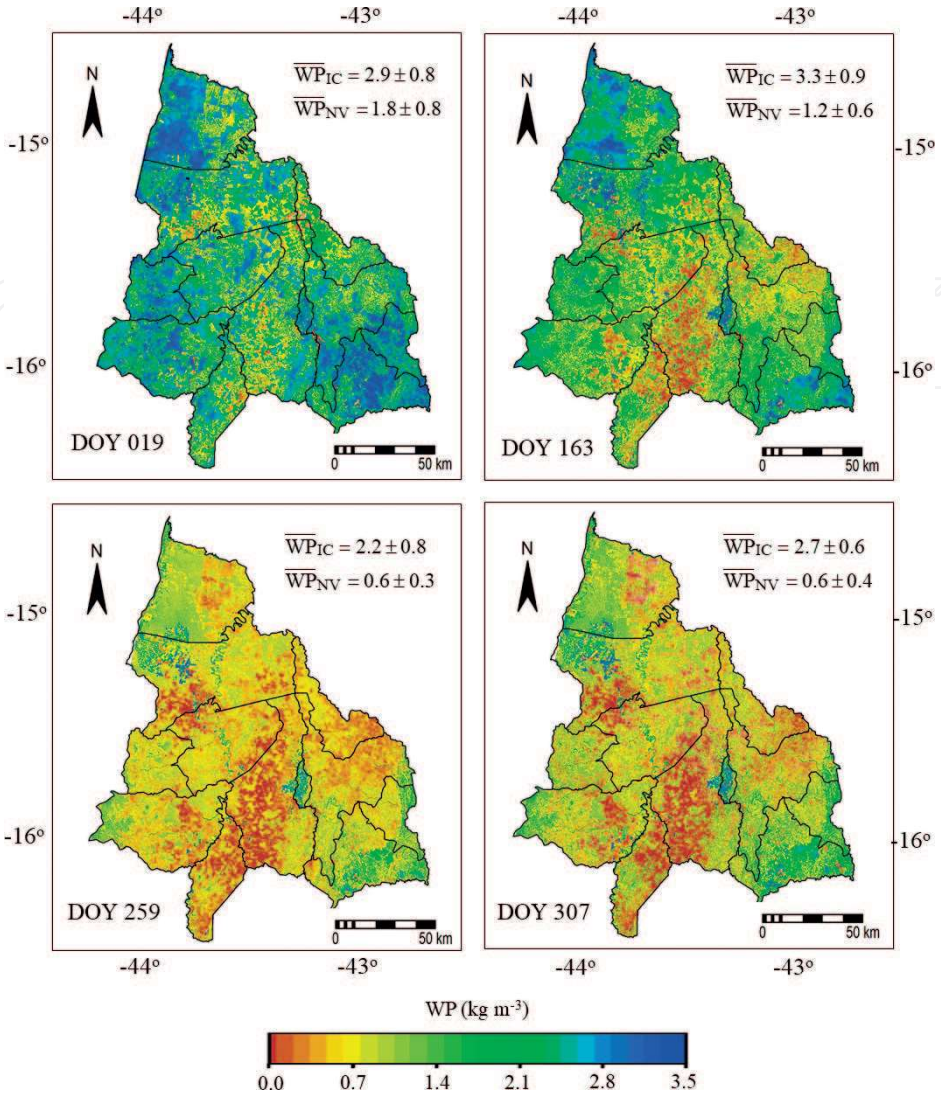

Figure 7. Spatial distribution of the daily values for the water productivity based on evapotranspiration (WP), under different hydrological conditions along the year 2015, in the north of Minas Gerais state, Southeast Brazil. DOY is the Day of the Year and the over bars means averages in irrigated crops (IC) and natural vegetation (NV) agroecosystems, showed together with the standard deviation (SD).

4. Conclusions

The coupled use of Landsat 8 images and a net of agrometeorological stations allowed the large-scale quantification of the water productivity parameters, under different hydrological conditions and agroecosystems during the year 2015 in the north of Minas Gerais state, Southeast Brazil. The analyses may subsidize a better understanding of the soil moisture, actual evapotranspiration (ET) and biomass production (BIO) dynamics, important water policy issues under the actual climate and land-use change conditions in the Brazilian semiarid region.

Vegetated surfaces were classified into irrigated crops (IC) and natural vegetation (NV), highlighting the rainy period as the one with the highest actual evapotranspiration (ET) and biomass production (BIO) rates for both irrigated crops (IC) and natural vegetation (NV) agroecosystems.

However, the largest water productivity based on evapotranspiration (WP) values, considered as the ratio of biomass production (BIO) to actual evapotranspiration (ET), was during the rainy period for the natural species, while for the irrigated crops they were soon after this period.

The remote sensing model algorithms applied here demonstrated enough accuracy to be implemented in rational water resource policies in the Brazilian semiarid region experiencing climate and land use changes, once having available spatially distributed agrometeorological data. From the sensibility of the models to detect soil moisture conditions, the results revealed confidence for later applications of monitoring water and vegetation indices, quantifying the effects of water scarcity along the years.

Acknowledgements

The National Council for Scientific and Technological Development (CNPq) is acknowledged for the financial support to a project on large-scale water productivity analyses in Brazil.

Author details

Antônio Heriberto de Castro Teixeira[1]*, Fúlvio R. Simão[2], Janice F. Leivas[3], Reinaldo L. Gomide[4], João B.R. da S. Reis[2], Mauro K. Kobayashi[5] and Flávio G. Oliveira[6]

*Address all correspondence to: heriberto.teixeira@embrapa.br

1 Embrapa Coastal Tablelands, Aracaju-SE, Brazil

2 Minas Gerais Agricultural Research Institute, Belo Horizonte/Nova Porteirinha-MG, Brazil

3 Embrapa Satellite Monitoring, Campinas-SP, Brazil

4 Embrapa Maize and Sorghum, Sete Lagoas-MG, Brazil

5 Montes Claros University, Janaúba-MG, Brazil

6 Minas Gerais Federal University, Montes Claros-MG, Brazil

References

[1] Companhia de Desenvolvimento dos Vales do São Francisco e Parnaíba - CODEVASF. Jaíba [Internet]. Available from: http://www.codevasf.gov.br/principal/perimetros-irrigados/elenco-de-projetos/jaiba-ii-iii-iv [Accessed: 2017-06-06]

[2] Leivas JF, Teixeira AH de C, Bayma-Silva G, Ronquim CC, Reis JBR da S. Biophysical indicators based on satellite images in an irrigated area at the São Francisco river basin, Brazil. Proceedings of SPIE. 2016;**9998**:99981N-99981N. DOI: 10.1117/12.2241320

[3] Teixeira AH de C, Leivas JF, Hernandez FBT, Franco RAM. Large-scale radiation and energy balances with Landsat 8 images and agrometeorological data in the Brazilian semiarid region. Journal of Applied Remote Sensing. 2017;**11**:016030. DOI: http://dx.doi.org/10.1117/1.JRS.11.016030

[4] Teixeira AH de C, Bastiaanssen WGM, Ahmad Mud D, Bos MG, Moura MSB. Analysis of energy fluxes and vegetation-atmosphere parameters in irrigated and natural ecosystems of semi-arid Brazil. Journal of Hydrology. 2008;**362**:110-127. DOI: http://dx.doi.org/10.1016/j.jhydrol.2008.08.01

[5] Teixeira AH de C. Determining regional actual evapotranspiration of irrigated and natural vegetation in the São Francisco river basin (Brazil) using remote sensing and penman-Monteith equation. Remote Sensing. 2010;**2**:1287-1319. DOI: 10.3390/RS0251287

[6] Monteith JL. Solar radiation and productivity in tropical ecosystems. Journal of Applied Ecology. 1972;**9**:747-766. DOI: http://dx.doi.org/10.2307/2401901

[7] Teixeira AH de C, Scherer-Warren M, Hernandez FBT, Andrade RG, Leivas JF. Large-scale water productivity assessments with MODIS images in a changing semi-arid environment: A Brazilian case study. Remote Sensing. 2013;**5**:55783-5804. DOI: 10.3390/rs5115783

[8] Teixeira AH de C, Hernandez FBT, Scherer-Warren M, Andrade RG, Victoria D de C, Bolfe EL, Thenkabail PS, Franco RAM. Water productivity studies from earth observation data: Characterization, modeling, and mapping water use and water productivity. In: Prasad ST, editor. Remote Sensing of Water Resources, Disasters, and Urban Studies. 1st ed. Boca Raton, Florida: Taylor and Francis, 2015, v. III, pp. 101-126. ISBN: 9781482217919

[9] Instituto Estadual de Florestas—IEF. Cobertura vegetal de Minas Gerais [Internet]. Available from: http://www.ief.mg.gov.br/florestas. [Accessed: 2017-06-06]

[10] Instituto Mineiro de Gestão das Águas—IGAM. Mapa UPGRH de Minas Gerais [Internet]. Available from: http://www.igam.mg.gov.br/images/stories/mapoteca/upgrhs-minas-gerais.pdf. [Accessed: 2017-06-06]

[11] Lumbreras JF, Naime UJ, Oliveira AP de, Silva Neto LF da, Carvalho Filho A de, Motta PEF da, Calderano SB, Simão MLR, Áglio MLD, Vieira EM, Machado ML, Santos AJR dos, Silva DC da, Souza JS de, Ferreira AR. Levantamento semi detalhado dos solos do Projeto Jaíba (Etapa III), Estado de Minas Gerais. Dados eletrônicos. Rio de Janeiro, Embrapa Solos, 2014, 148 p. (Boletim de pesquisa e desenvolvimento No. 248/Embrapa Solos, ISSN: 1678-0892)

[12] Vanhellemont Q, Kevin Ruddick K. Turbid wakes associated with offshore wind turbines observed with Landsat 8. Remote Sensing of Environment. 2014;**45**:105-115. http://dx.doi.org/10.1016/j.rse.2014.01.009

[13] Raupasch MR. Combination theory and equilibrium evaporation. Quarterly Journal of Royal Meteorological Society. 2001;**127**:1149-1181. http://dx.doi.org/10.1002/qj.49712757402

[14] Bastiaanssen WGM, Ali S. A new crop yield forecasting model based on satellite measurements applied across the Indus Basin, Pakistan. Agriculture, Ecosystem and Environments. 2003;**94**:32-340. http://dx.doi.org/10.1016/S0167-8809(02)00034-8

[15] Teixeira AH de C, Tonietto J, Leivas JF. Large-scale water balance indicators for different pruning dates of tropical wine grape. Pesquisa Agropecuária Brasileira. 2016;**51**:849-857. http://dx.doi.org/10.1590/S0100-204X2016000700008

[16] Lu N, Chen S, Wilske B, Sun G, Chen J. Evapotranspiration and soil water relationships in a range of disturbed and undisturbed ecosystems in the semi-arid Inner Mongolia, China. Journal of Plant Ecology. 2011;**4**:49-60. https://doi.org/10.1093/jpe/rtq035

[17] Zhang F, Zhou G, Wang Y, Yan F, Christer Nilsson C. Evapotranspiration and crop coefficient for a temperate desert steppe ecosystem using eddy covariance in Inner Mongolia, China. Hydrological Processes. 2012;**26**:379-386. DOI: 10.1002/hyp.8136

[18] Sumner DM, Jacobs J. Utility of penman-Monteith, Priestley-Taylor, reference evapotranspiration, and pan evaporation methods to estimate pasture evapotranspiration. Journal of Hydrology. 2005;**308**:81-104. DOI: 10.1016/j.jhydrol.2004.10.023

[19] Zhou L, Zhou G. Measurement and modeling of evapotranspiration over a reed (*Phragmites australis*) marsh in Northeast China. Journal of Hydrology. 2009;**372**:41-47. DOI: 10.1016/j.jhydrol.2009.03.033

[20] Mata-González R, McLendon T, Martin DW. The inappropriate use of crop transpiration coefficients (K_c) to estimate evapotranspiration in arid ecosystems: A review. Arid Land Research and Management. 2005;**19**:285-295. http://dx.doi.org/10.1080/15324980590951469

[21] Teixeira AH de C. Modelling water productivity components in the Low-Middle São Francisco River basin, Brazil. In: Bilibio C, Hensel O, Selbach J, editors. Sustainable Water Management in the Tropics and Subtropics and Case Studies in Brazil. Kassel: University of Kassel; 2012